

## Frequency dependence of capnography in anesthetized rabbits

I. Ioan<sup>a</sup>, B. Demoulin<sup>b</sup>, C. Duvivier<sup>b</sup>, A.L. Leblanc<sup>b</sup>, C. Bonabel<sup>a</sup>, F. Marchal<sup>a,b,\*</sup>,  
C. Schweitzer<sup>a,b</sup>, S. Varechova<sup>a,b</sup>

<sup>a</sup> Service d'explorations fonctionnelles pédiatriques, Hôpital d'Enfants, CHU de Nancy, France

<sup>b</sup> EA 3450, Laboratoire de Physiologie, Faculté de Médecine, Université de Lorraine, France

### ARTICLE INFO

#### Article history:

Received 26 April 2013

Received in revised form 4 September 2013

Accepted 4 September 2013

#### Keywords:

Forced oscillations

Asthma

Methacholine

Bronchoconstriction

Artificial ventilation

Expired CO<sub>2</sub>

### ABSTRACT

Aspirative capnography may be of help to diagnose early childhood asthma, but clinical usefulness in young children is limited by the relatively high respiratory rate. This study aimed to characterize the F<sub>CO<sub>2</sub></sub> time course during airway constriction in 8 anesthetized rabbits, artificially ventilated at 30, 60 and 80 breaths/min. Methacholine was inhaled to double the respiratory resistance measured at 8 Hz by the forced oscillation technique. The capnogram shape changed in response to both methacholine and ventilatory frequency. Slope of phase II, the peak of first-order time derivative and trough of the second-order time derivative of the F<sub>CO<sub>2</sub></sub> signal, were significantly attenuated after methacholine compared with baseline at all breathing rates ( $p < 0.02$ ). Moreover, significant correlations between respiratory reactance and resistance were observed with the phase III slope and the angle described by phase II and phase III ( $p < 0.01$ ). It is concluded that capnography may be useful to identify acute airway changes related to bronchoconstriction, even at high breathing frequencies.

© 2013 Elsevier B.V. All rights reserved.

### 1. Introduction

The accurate diagnostic of early childhood asthma is critical because delayed recognition of the disease may result in repeated exacerbations and chronic airway obstruction that may eventually lead to airway remodeling (Elias et al., 1999; Canonica, 2006; Grainge et al., 2011). Lung function testing is an important adjunct to medical history and physical examination as an objective assessment of airway obstruction and/or hyperresponsiveness. A number of techniques have been developed during the recent years that involve only minimal cooperation from the subject and are therefore ideally suited to early childhood. The multiple-breath washout of inert gases or of nitrogen by oxygen identifies the contribution of inhomogeneous ventilation to the obstructive lung disease (Gustafsson, 2005). The lung clearance index has thus been shown to be an early detector of lung function abnormalities in cystic fibrosis (Gustafsson, 2005; Robinson et al., 2010). With either method however, an airtight mask-to-face seal is mandatory for valid interpretation, and sedation may be required beyond a few months of age.

When toddlers or young children are hospitalized during an acute asthma episode, non invasive – non disturbing estimation of the airway obstruction may be of significant help for both

diagnostic and management, if possible at the bedside. Indeed, even washout techniques are challenging as they require a laboratory environment and the subject may poorly tolerate contact with the face mask and instrumental dead space. Analysis of how the shape of the expired CO<sub>2</sub> time course is altered by the non homogeneous distribution of ventilation resulting from the bronchoconstriction may be a valuable alternative. It is achievable during spontaneous breathing, without sedation or additional deadspace, but at the expense of a small sample-line inserted a few millimeters deep into a nostril. The capnogram may be characterized from a number of indices that reflect the relevant parts of the S shaped expired CO<sub>2</sub> profile (You et al., 1994). During heterogeneous airway obstruction, the asynchronous emptying of alveolar territories leads to more gradual CO<sub>2</sub> front at the transition from dead space to alveolar volume as well as a steeper tele-expiratory plateau.

Young children and toddlers have a relatively elevated rate of breathing that may increase further during an acute respiratory exacerbation. This may impact on the measurement of expired CO<sub>2</sub> indices mainly as a result of the measuring apparatus response time. In this condition, the advantage of the aspirative capnography may be offset by a fast rate of breathing. To the best of our knowledge, little data are available on the validity of capnographic indices as a detector of airway obstruction in a range of breathing frequencies relevant to acute pediatric asthma.

The primary objective of the study was therefore to characterize the change in capnogram indices induced by acute airway obstruction at different rates of breathing, with reference to established markers of respiratory mechanics, such as respiratory resistance

\* Corresponding author at: Service d'explorations fonctionnelles pédiatriques, Hôpital d'Enfants, CHU de Nancy, France. Tel.: +33 383154795; fax: +33 383154798.  
E-mail address: [f.marchal@chu-nancy.fr](mailto:f.marchal@chu-nancy.fr) (F. Marchal).

(Rrs) and reactance (Xrs) assessed by the forced oscillations technique (FOT). Because the study may be difficult to achieve in a standardized way in clinical conditions, measurements were performed in artificially ventilated rabbits. While it may be argued that extrapolation of physiologic findings in artificially ventilated adult rabbits to spontaneously breathing young children may not be straightforward, it is believed that the consequences of acute airway obstruction constriction – such as the impact of a change in smooth muscle tone and its distribution throughout the lung – may be studied using this animal model in a range of breathing rates and ventilations relevant to young children.

## 2. Materials and methods

### 2.1. Animals

Eight New Zealand adult rabbits (weight mean  $\pm$  SD:  $3.1 \pm 0.4$  kg) were studied. Animal housing and experiments were performed according to the recommendations 86-609 CEE issued by the Council of the European communities and under licenses from the “Ministère de l’Agriculture et de la Pêche” and the “Ministère de l’Enseignement Supérieur et de la Recherche” (A54518-03409) and supervision by the “Services Vétérinaires Départementaux de Meurthe et Moselle”.

### 2.2. General and respiratory mechanics

The spontaneously breathing animal was placed on a heating pad, anaesthetized with a loading dose of sodium Pentobarbital (25 mg/kg) injected through an ear vein. Supplemental doses (2.5 mg/kg) were given every 30 min. The trachea was incised, intubated and connected to a Fleisch No. 0 pneumotachograph to measure airflow. The rabbits were mechanically ventilated, and paralyzed with pancuronium bromide (0.2 mg/kg), which was repeated when spontaneous respiratory efforts were detected. The artificial ventilation was set at 3 different rates of breathing: 30, 60 and 80 cycles/min, and the tidal volume was varied in order to maintain a quasi-constant ventilation, so as to minimize the change in alveolar  $P_{CO_2}$ .

Transrespiratory pressure was generated by a loudspeaker as a sine wave forcing signal at 8 Hz, and measured at a side port of the tracheal cannula. Respiratory resistance (Rrs) and reactance (Xrs) were computed oscillation, per oscillation, respectively as the real and imaginary part of the complex ratio of transrespiratory pressure to flow. The expiration of each breathing cycle was examined to select the respiratory impedance value closest to zero flow, so as to minimize the flow dependence of Rrs that is expected to become more apparent when breathing rate increases (Schweitzer et al., 2006).

### 2.3. Capnography

The respired gas was sampled through a 1 mm ID 100 cm length catheter with an aspiration flow of 200 mL/min, and fed to an Infrared Carbon Dioxide Analyzer (Vacumed # 17630  $CO_2$  Analyzer, Silver Edition Ventura, CA, USA). Transit and rise times – checked *in vitro* using a bolus gas mixture containing 5%  $CO_2$  – had been determined to be respectively 431 ms and 150 ms. The sampling line was connected to the tracheal cannula through one arm of a Y tube, the other arm of which was attached to the ventilator. Following analysis, the sampled gas was reinjected into the ventilator circuit.

The expired  $CO_2$  time course illustrated in Fig. 1 displays the typical S shape pattern: expiration of gas from dead space (phase I), transition from dead space to alveolar gas (phase II) and slightly ascending end expiratory plateau of alveolar gas (phase III). The

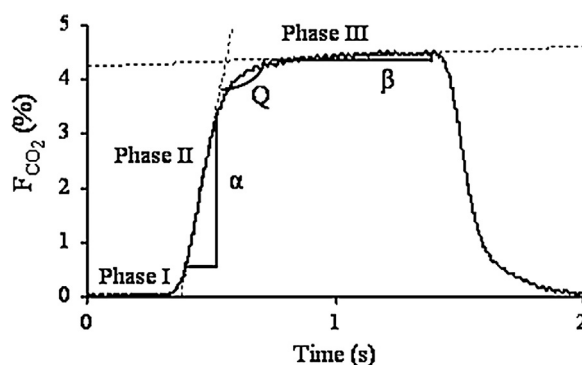


Fig. 1. Typical capnogram showing expiration of gas from dead space (Phase I); transition from dead space to alveolar volume (Phase II) and end expiratory (alveolar) plateau (Phase III).  $F_{CO_2}$ :  $CO_2$  fraction in the respired gas;  $\alpha$  and  $\beta$ : estimated slope of phase II and phase III;  $Q$ : angle between  $\alpha$  and  $\beta$ .

S is then followed by the prompt  $F_{CO_2}$  decrease with inspiration. Five indices were computed to describe the flattening of the capnogram, expected from the bronchoconstriction. The slope of the  $F_{CO_2}$  vs time regression line ( $\alpha$ ) was computed between 10% and 70% of the end tidal  $F_{CO_2}$ . This interval was retained because the analyzer rise time is computed within this  $F_{CO_2}$  range that excludes transitions from phase I to phase II and from phase II to phase III. The corresponding time interval is thus expected to allow the most accurate computation of  $\alpha$ . For the computation of phase III slope ( $\beta$ ), the peak time derivatives of the capnogram ascending and descending limbs were projected orthogonally to determine a time interval from which the early 30% and late 20% were excluded. The algorithm had been empirically determined so as to include – at each frequency of interest – the optimal number of points most significantly contributing to the alveolar slope, i.e., including the most linear part and excluding transitions from phase II to phase III and from phase III to the descending limb. The transition from phase II to III was characterized by its angle of curvature ( $Q$ ) computed using  $\alpha$ ,  $\beta$  and trigonometric relationships. The instantaneous first- and second-order time derivatives were calculated and low-pass filtered at 20 Hz. The first peak of the first-order derivative ( $F'_{CO_2}$ , Fig. 2) and the first trough of the second-order derivative ( $F''_{CO_2}$ , Fig. 3) were retained for analysis.  $F'_{CO_2}$  is another way to characterize phase II and  $F''_{CO_2}$  expresses mostly the curvature at the transition from  $\alpha$  to  $\beta$ , with the potential advantage that these computations are unbiased, in contrast with slope or angle analysis that require selecting an interval within a series to be analyzed. Slopes and time derivatives were expressed as raw values and also normalized to the end-tidal  $CO_2$  that was observed to decrease usually with increased breathing frequency.

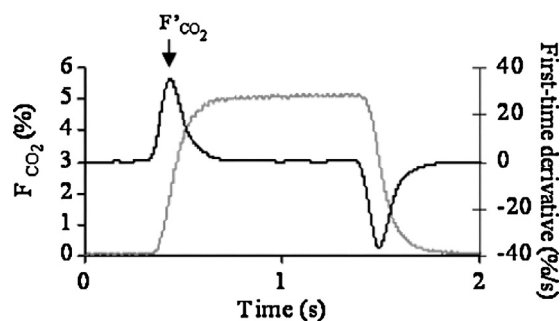


Fig. 2. Time course of the  $F_{CO_2}$  first-order time derivative (dark line) is superimposed on the capnogram (gray line). At arrow,  $F'_{CO_2}$  indicates peak of the first-order time derivative value. Abbreviations as in Fig. 1.

Download English Version:

<https://daneshyari.com/en/article/2847109>

Download Persian Version:

<https://daneshyari.com/article/2847109>

[Daneshyari.com](https://daneshyari.com)